Electrochemical oxidation of chalcopyrite (CuFeS$_2$) and the related metal-enriched derivatives Cu$_4$Fe$_5$S$_8$, Cu$_9$Fe$_9$S$_{16}$, and Cu$_9$Fe$_8$S$_{16}$

D. J. Vaughan, K.E.R. England
Department of Geology, University of Manchester, Manchester M13 9PL, U.K.

G. H. Kelsall, Q. Yin
Department of Mineral Resources Engineering, Imperial College, London SW7 2BP, U.K.

Abstract

The electrochemical oxidation of chalcopyrite (CuFeS$_2$) and its metal-enriched derivatives, haycockite (Cu$_4$Fe$_5$S$_8$), mooihoekite (Cu$_9$Fe$_9$S$_{16}$), and talnakhite (Cu$_9$Fe$_8$S$_{16}$), have been investigated using electrochemical techniques and X-ray photoelectron spectroscopy. The results show that when chalcopyrite, haycockite, mooihoekite, and talnakhite are oxidized in 1 M HClO$_4$ in the electrode potential region of 0.2–0.6 V vs. S.C.E. at 298 K, the oxidation products are Cu$_x$S$_z^*$, Fe^{2+} and, at electrode potentials > 0.53 V vs. S.C.E., Fe^{3+} ions; Cu$_x$S$_z^*$ represents a metastable phase at the electrode surface. The relative rates of oxidation are in the order haycockite > mooihoekite > talnakhite > chalcopyrite. After oxidation of Fe surface sites, the rate-determining step apparently involves transport of Fe ions from the bulk to the solid-electrolyte interface. When chalcopyrite, haycockite, mooihoekite, and talnakhite are oxidized in 0.1 M borax in the electrode potential range of −0.6–0.3 V vs. S.C.E. at 298 K, the primary oxidation products are Cu$_x$S$_z^*$ and Fe$_2$O$_3$. The initial oxidation rates of haycockite, mooihoekite, and talnakhite are higher than chalcopyrite, but this initially more facile oxidation of haycockite, mooihoekite, and talnakhite results in metal oxide (mainly iron oxide) surface films, which retard further oxidation to a greater extent than on chalcopyrite. When chalcopyrite, haycockite, mooihoekite, and talnakhite are oxidized in 0.3 M NaCl + HCl solution of pH 0.1, the oxidation rates remain essentially in the order haycockite > mooihoekite > talnakhite > chalcopyrite. However, probably because chloride ions form complexes with Cu$^+$ ions and may act as a bridge in electron transfer, the oxidation rate is significantly enhanced compared to that in 1 M perchloric acid and 0.1 M borax aqueous solutions.

Introduction

Chalcopyrite is the most important Cu-bearing ore mineral. To develop more efficient technological processes for Cu concentration and extraction involving froth flotation and hydrometallurgical methods, the electrochemical behavior of chalcopyrite in aqueous solutions has been widely investigated.

Jones (1974) and Jones and Peters (1976a, 1976b) proposed that covellite is the phase formed on the surface in the low current density region and responsible for passivation during the anodic dissolution of chalcopyrite. Warren (1978) and Warren et al. (1982, 1983) observed that the initial anodic decomposition of chalcopyrite resulted in formation of an intermediate product phase Cu$_{1-x}$Fe$_{1-y}$S$_{2-z}$, mixed with S, both of which retard further oxidation. Page (1988) considered that the pre-wave process may involve the oxidation of chalcopyrite to covellite (CuS) through CuFe$_{0.2}$S$_{0.8}$ and Cu$_2$S as intermediates.

Ammou-Chokroum et al. (1977, 1978, 1981) proposed a mechanism involving the formation of CuS to explain the decrease in electro-dissolution rate. McMillan et al.

(1982) interpreted anodic passivation as being caused by a solid electrolyte interphase, which slowed the rate of electron transfer. Holliday and Richmond (1990) showed that as chalcopyrite is dissolved anodically in acidic solutions, the initial rate-determining step is the production of adsorbed Cu^{2+} ions and then Fe^{2+} ions. The final ratio of aqueous Fe^{2+} to Cu^{2+} produced was determined as 5:1.

Reports of experiments carried out in alkaline solutions are far fewer than in acidic solutions. Gardner and Woods (1979) suggested that the oxidation reaction of chalcopyrite in alkaline solutions produces CuS, Fe(OH)$_3$, and S. They considered that the presence of S on the mineral surface is the critical factor in rendering chalcopyrite floatable. Page (1988) proposed that in the oxidation of chalcopyrite in alkaline solution, chalcopyrite is first oxidized to Cu$_2$S, Fe(OH)$_3$, and S; then Cu$_2$S is oxidized to S and CuS, which is oxidized further to S and Cu(OH)$_2$. Dean (1991) found that at electrode potentials < 0.4 V vs. saturated calomel reference electrode (S.C.E.), a homogeneously distributed oxide film of a composition similar to CuFe$_2$O$_4$ is formed on metal-depleted chalcopyrite, the presence of copper oxide on chalcopyrite being

evident only at electrode potentials > 0.4 V vs. S.C.E. at pH 9.2.

In industry, it has been found that chalcopyrite from different sources may display very different behavior during froth flotation or during bacterial and chemical leaching. Besides the possible effects of minor elements in the minerals, subtle variations in stoichiometry could well be a cause of such differences. Therefore, it is of interest to study the oxidation rates of Cu-Fe-S compounds with both the exact and approximate compositions of chalcopyrite and to make comparisons between them.

Before the late 1960s, some minerals with apparently metal-rich compositions compared to chalcopyrite but very similar properties (Vaughan and Craig, 1978) had been noted, but none of those minerals had been well characterized. In 1967, Cabri (1967) found and characterized a new copper-iron sulfide, talnakhite ($Cu_9Fe_8S_{16}$); subsequently, Cabri and Hall (1972) found and characterized two other sulfides, haycockite ($Cu_4Fe_5S_8$) and mooihoekite ($Cu_9Fe_9S_{16}$). In these so called stuffed derivatives of chalcopyrite, additional metal atoms occupy normally empty sites in the structure with primary coordination to four S atoms but with six other metal atoms at relatively close distances. To our knowledge, no work has been reported on the electrochemical oxidation of talnakhite ($Cu_9Fe_8S_{16}$), haycockite ($Cu_4Fe_5S_8$), and mooihoekite ($Cu_9Fe_9S_{16}$). In the present work, electrochemical techniques and X-ray photoelectron spectroscopy (XPS) have been employed to investigate the oxidation behavior of chalcopyrite ($CuFeS_2$) and its stuffed derivatives, haycockite ($Cu_4Fe_5S_8$), mooihoekite ($Cu_9Fe_9S_{16}$), and talnakhite ($Cu_9Fe_8S_{16}$) in different electrolytes and at various electrode potentials. Clear differences in electrochemical oxidation behavior, particularly in the lower anodic potential region, were found and are discussed below.

EXPERIMENTAL METHODS

Samples of chalcopyrite ($CuFeS_2$), haycockite ($Cu_4Fe_5S_8$), mooihoekite ($Cu_9Fe_9S_{16}$), and talnakhite ($Cu_9Fe_8S_{16}$) were synthesized using sealed, evacuated silica tube techniques (Vaughan and Craig, 1978) and employing high-purity (99.999 wt%) powders of elemental Cu, Fe, and S. Reflected light microscopy, wavelength dispersive electron microprobe analysis, and X-ray diffraction were employed to characterize the synthesized samples. Electrodes were prepared from the characterized samples and mounted in epoxy resin. They were ground with SiC paper down to 1200 grade, then polished with 0.3 and 0.05 μm alumina, screw mounted onto a threaded epoxy resin holder on the end of a glass tube containing the Cu connecting wire, and electrical connection established through a small brass disc in contact with the Au-sputtered back surface of the mineral. The mounted electrode was then washed with deoxygenated deionized water to remove any adhering alumina particles.

Three kinds of electrolyte were prepared using analyt-

ical grade perchloric acid, hydrochloric acid, or borax with deionized water of resistivity > 6.3×10^5 ohm·m: 1 M perchloric acid (pH 0), 0.1 M borax (pH 9.2), and 0.3 M NaCl + HCl (pH 0.1). The electrochemical experiments were carried out in a three-compartment cell, incorporating a Pt flag counter electrode and S.C.E., against which all electrode potentials quoted in this paper are reported. The cell was placed in a thermostatically controlled water bath at 25 ± 0.5 °C, at least 1 h prior to the experiments. Electrode potential control was achieved with a Princeton Applied Research 273 Potentiostat-Galvanostat, itself controlled by an IBM compatible microcomputer.

After the electrochemical experiments had been carried out, some of the oxidized electrodes were carefully transferred into a Kratos XSAM 800 surface analysis system to characterize surface compositions. The instrument was calibrated using the peaks: Au $4f_{7/2}$ 83.98 eV, Cu $2p_{3/2}$ 932.67 eV, Ag $3d_{5/2}$ 368.27 eV and with $MgK\alpha$ X-rays as the exciting radiation. Electron spectra were recorded at an analyzer pass energy of 20 eV. The static charge effect was corrected using adventitious C with the 1s electron binding energy taken as 284.6 eV. From final polishing of electrodes to transfer into the surface analysis system, all operations were carried out in an O_2-free N_2 environment.

RESULTS AND DISCUSSION

Linear potential sweep voltammetry

The voltammograms shown in Figure 1 were obtained in 1 M $HClO_4$ in the electrode potential region of 0.2–0.6 V vs. S.C.E. In the figure, curves A, B, C, and D represent the polarization curves of haycockite, mooihoekite, talnakhite, and chalcopyrite, respectively. This indicates that, before commencement of the active oxidation at the high electrode potential region, there is a pre-wave region (0.2–0.6 V vs. S.C.E.) in which the oxidation processes occur at different rates. Of the four phases studied, $CuFeS_2$ was oxidized at the lowest rate with an oxidation current density of ~0.1 mA/cm². Haycockite was the most reactive, the oxidation current density being ~1.5 mA/cm². Mooihoekite and talnakhite are intermediate in reactivity, the oxidation current densities being about 0.8 and 0.5 mA/cm², respectively. In this electrode potential region, the primary reaction may be

$$Cu_xFe_yS_z \rightarrow Cu_xS_z^* + yFe^{2+} + 2ye^- \qquad (1)$$

$$Cu_xFe_yS_z \rightarrow Cu_xS_z^* + yFe^{3+} + 3ye^- \qquad (2)$$
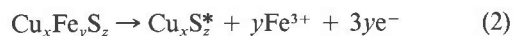
where x, y, and z are positive integers, and $Cu_xS_z^*$ represents a metastable phase at the electrode surface forming a passive film. The differences in the oxidation rates may be primarily attributed to extra stuffed metal atoms in haycockite, mooihoekite, and talnakhite, with the extra metal atoms being located in the unoccupied set of tetrahedral sites of the cubic close-packed S lattice. When the electrode potential is increased to >0.7 V vs. S.C.E., the oxidation current density increases abruptly, indicating that the following reactions may take place:
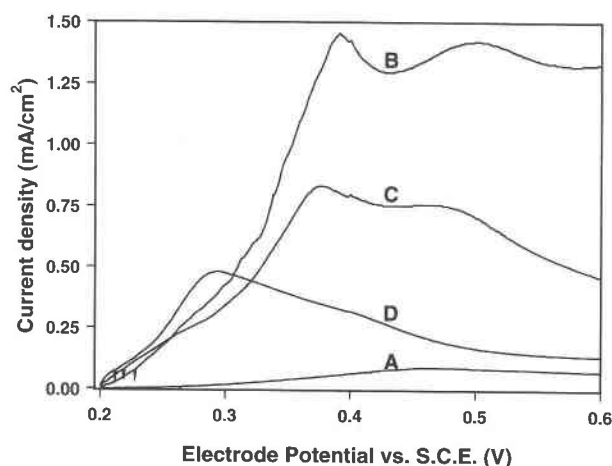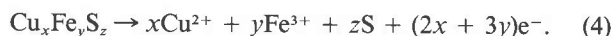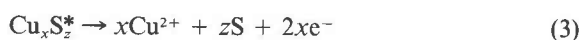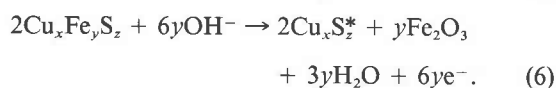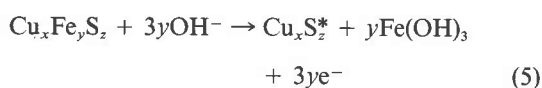
Fig. 1. Linear potential sweep voltammograms of Cu-Fe-S compounds in 1 M HClO$_4$ at 298 K; electrode potential sweep rate: 20 mV/s: (A) haycockite; (B) mooihoekite; (C) talnakhite; (D) chalcopyrite.

Fig. 2. Linear potential sweep voltammograms of Cu-Fe-S compounds in 0.1 M Na$_2$B$_4$O$_7$ at 298 K; electrode potential sweep rate: 20 mV/s: (A) chalcopyrite; (B) haycockite; (C) mooihoekite; (D) talnakhite.

$$Cu_xS_z^* \rightarrow xCu^{2+} + zS + 2xe^- \qquad (3)$$

$$Cu_xFe_yS_z \rightarrow xCu^{2+} + yFe^{3+} + zS + (2x + 3y)e^-. \qquad (4)$$

The voltammograms shown in Figure 2 were obtained in 0.1 M Na$_2$B$_4$O$_7$ (pH 9.2) in the electrode potential range of -0.6–0.6 V vs. S.C.E. Curves A, B, C, and D represent polarization curves for chalcopyrite, haycockite, mooihoekite, and talnakhite, respectively. They indicate that before the main oxidation current (density) peak, there is again a pre-wave region (-0.6 V to $+0.3$ V vs. S.C.E.). The corresponding reactions may be as follows:

$$Cu_xFe_yS_z + 3yOH^- \rightarrow Cu_xS_z^* + yFe(OH)_3$$
$$+ 3ye^- \qquad (5)$$

$$2Cu_xFe_yS_z + 6yOH^- \rightarrow 2Cu_xS_z^* + yFe_2O_3$$
$$+ 3yH_2O + 6ye^-. \qquad (6)$$

The voltammograms indicate that the anodic oxidation rates of haycockite, mooihoekite, and talnakhite are greater than that of chalcopyrite at an electrode potential lower than 0.22 V vs. S.C.E. However, with an electrode potential > 0.22 V vs. S.C.E., the opposite is observed. This may be because haycockite, mooihoekite, and talnakhite have extra metal atoms that are easier to transport through the lattice, enabling them to be readily oxidized anodically. However, this initially more facile oxidation may result in a thicker and more compact metal oxide (mainly iron oxide) surface film, which retards further oxidation to a greater extent than on chalcopyrite.

When the electrode potential is increased to ca. 0.4 V vs. S.C.E., the following reactions may start to occur:
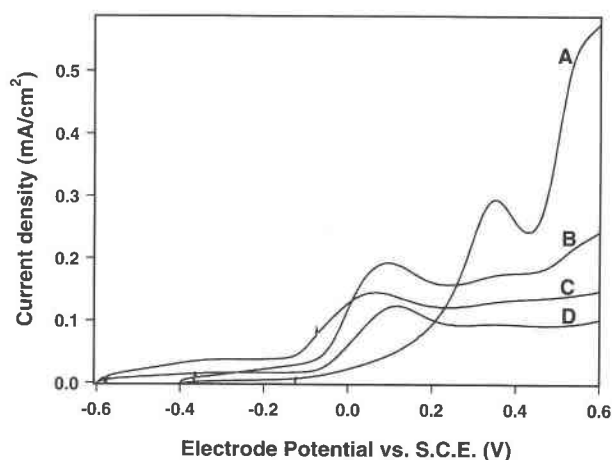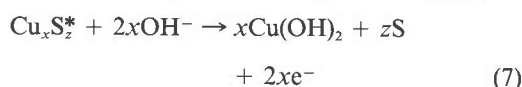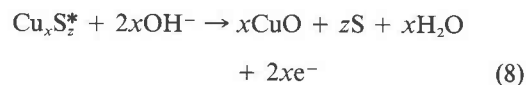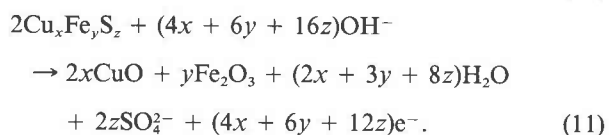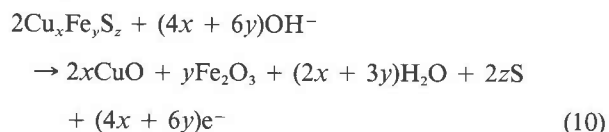
$$Cu_xS_z^* + 2xOH^- \rightarrow xCu(OH)_2 + zS$$
$$+ 2xe^- \qquad (7)$$

$$Cu_xS_z^* + 2xOH^- \rightarrow xCuO + zS + xH_2O$$
$$+ 2xe^- \qquad (8)$$

$$Cu_xS_z^* + (2x + 8z)OH^- \rightarrow xCuO + zSO_4^{2-}$$
$$+ (x + 4z)H_2O$$
$$+ (2x + 6z)e^- \qquad (9)$$

thereby enhancing the underlying chalcopyrite oxidation rate by the reactions

$$2Cu_xFe_yS_z + (4x + 6y)OH^-$$
$$\rightarrow 2xCuO + yFe_2O_3 + (2x + 3y)H_2O + 2zS$$
$$+ (4x + 6y)e^- \qquad (10)$$

$$2Cu_xFe_yS_z + (4x + 6y + 16z)OH^-$$
$$\rightarrow 2xCuO + yFe_2O_3 + (2x + 3y + 8z)H_2O$$
$$+ 2zSO_4^{2-} + (4x + 6y + 12z)e^-. \qquad (11)$$

It is obvious that, in the high electrode potential region, part of the S being oxidized to sulfate could make the passive film somewhat porous; but elemental S and metal oxides still remain on the electrode surface, and the passive film does not breakdown totally. Thus, the oxidation current density of the Cu-Fe-S compounds in alkaline solution is much smaller than in acid solution, even in the high electrode potential region, except for chalcopyrite. This exception may result from lack of extra interstitial metal atoms and a lower atomic ratio of metal to S in chalcopyrite.

The voltammograms obtained in a 0.3 M NaCl and HCl aqueous solution (pH 1) are shown in Figure 3, with electrode potentials being swept from open circuit values to 0.6 V vs. S.C.E. It can be seen that there is a quite large current (density) peak at an electrode potential around ~0.3 V vs. S.C.E., which is particularly evident
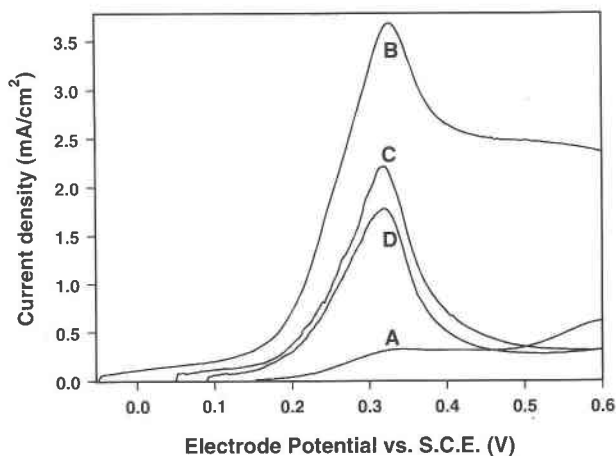
Fig. 3. Linear potential sweep voltammograms of Cu-Fe-S compounds in 0.3 M NaCl plus HCl solution (pH 0.1) at 298 K; electrode potential sweep rate: 20 mV/s: (A) chalcopyrite; (B) haycockite; (C) mooihoekite; (D) talnakhite.

Fig. 5. Current (density)–time transients in response to a step in electrode potential from rest potential to 0.4 V vs. S.C.E. in 0.1 M Na$_2$B$_4$O$_7$ at 298 K: (A) chalcopyrite; (B) haycockite; (C) mooihoekite.

for haycockite (curve B), mooihoekite (curve C), and talnakhite (curve D). The high oxidation rates in this electrolyte may be attributed primarily to the effects of chloride ions, which may act as a bridge in electron transfer and form Cu$^+$ complexes with the general formula CuCl$_m^{(m-1)-}$; these decrease the reversible electrode potential of the oxidation reaction, making it more facile relative to the behavior in the absence of such complexants. The initial anodic reactions may be attributed to
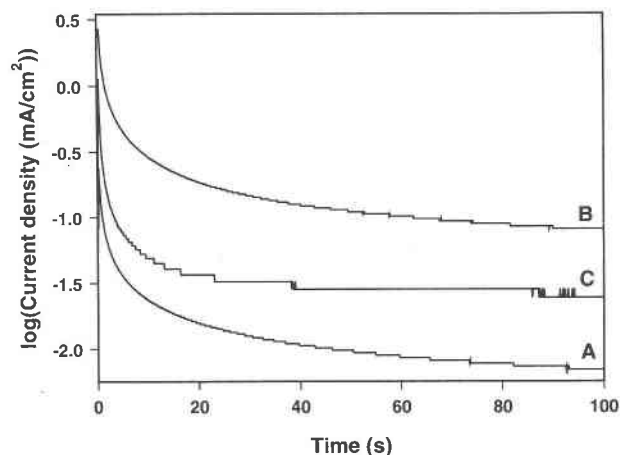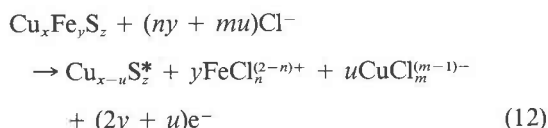
$$Cu_xFe_yS_z + (ny + mu)Cl^-$$
$$\rightarrow Cu_{x-u}S_z^* + yFeCl_n^{(2-n)+} + uCuCl_m^{(m-1)-}$$
$$+ (2y + u)e^- \qquad (12)$$

$$Cu_xFe_yS_z + (ny + mu)Cl^-$$
$$\rightarrow Cu_{x-u}S_z^* + yFeCl_n^{(3-n)+} + uCuCl_m^{(m-1)-}$$
$$+ (3y + u)e^- \qquad (13)$$

where n, m, and u, like x, y, and z, are positive integers with $u < x$.

Chronoamperometry

Figure 4 shows a set of current (density)–time transients in response to a step in electrode potential from rest value(s) to 0.3 V vs. S.C.E. in 1 M HClO$_4$. They indicate that the oxidation rates are in the order haycockite > mooihoekite > chalcopyrite, the same se-

Fig. 4. Current (density)–time transients in response to a step in electrode potential from rest potential to 0.3 V vs. S.C.E. in 1 M HClO$_4$ at 298 K: (A) haycockite; (B) mooihoekite; (C) chalcopyrite.
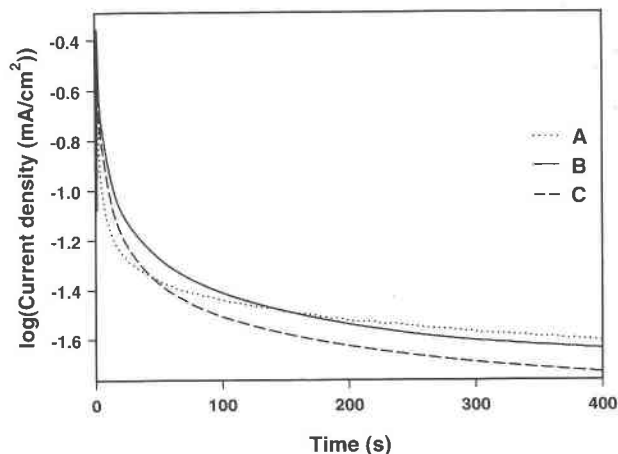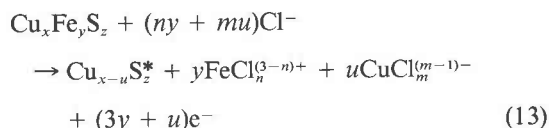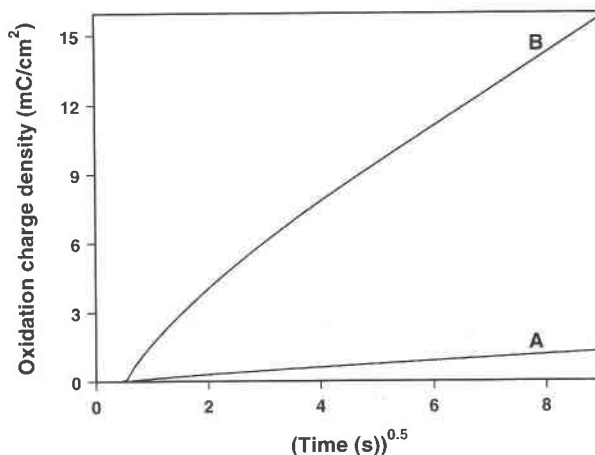

Fig. 6. Correlation between oxidation charge density and square root of time in 1 M HClO$_4$ at 298 K, when the electrode potential is stepped from rest to 0.3 V vs. S.C.E.: (A) haycockite; (B) chalcopyrite.
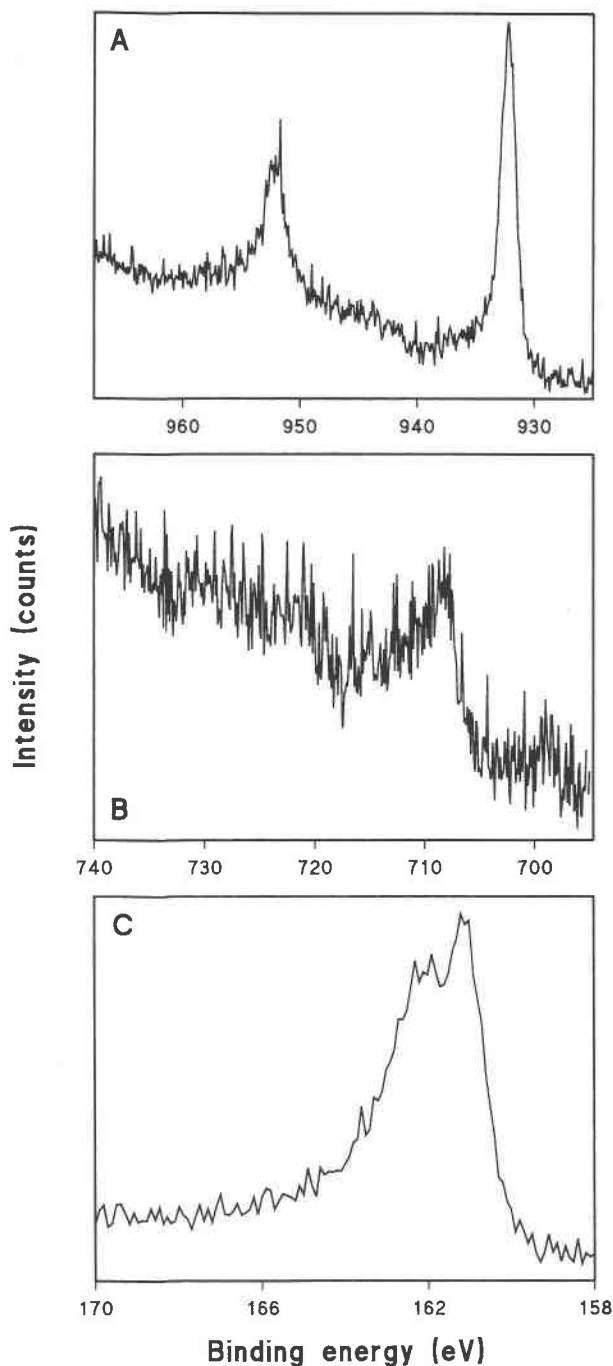
Fig. 7. XPS spectra from a chalcopyrite electrode surface oxidized in 1 M $HClO_4$ at 0.3 V vs. S.C.E. and 298 K: (A) Cu 2p; (B) Fe 2p; (C) S 2p. Charge density passed = 14.2 C/m² over 100 s.

Fig. 8. XPS spectra from haycockite electrode surface oxidized in 1 M $HClO_4$ at 0.3 V vs. S.C.E. and 298 K: (A) Cu 2p; (B) Fe 2p; (C) S 2p. Charge density passed = 174 C/m² over 100 s.

quence as was found by linear potential sweep voltammetry. Although the faster oxidation of haycockite and mooihoekite would lead to thicker passive layers, the oxidation rates remain in the order haycockite > mooihoekite > chalcopyrite during the whole oxidation process, implying that the passivation of haycockite and mooihoekite is less extreme than that of chalcopyrite.
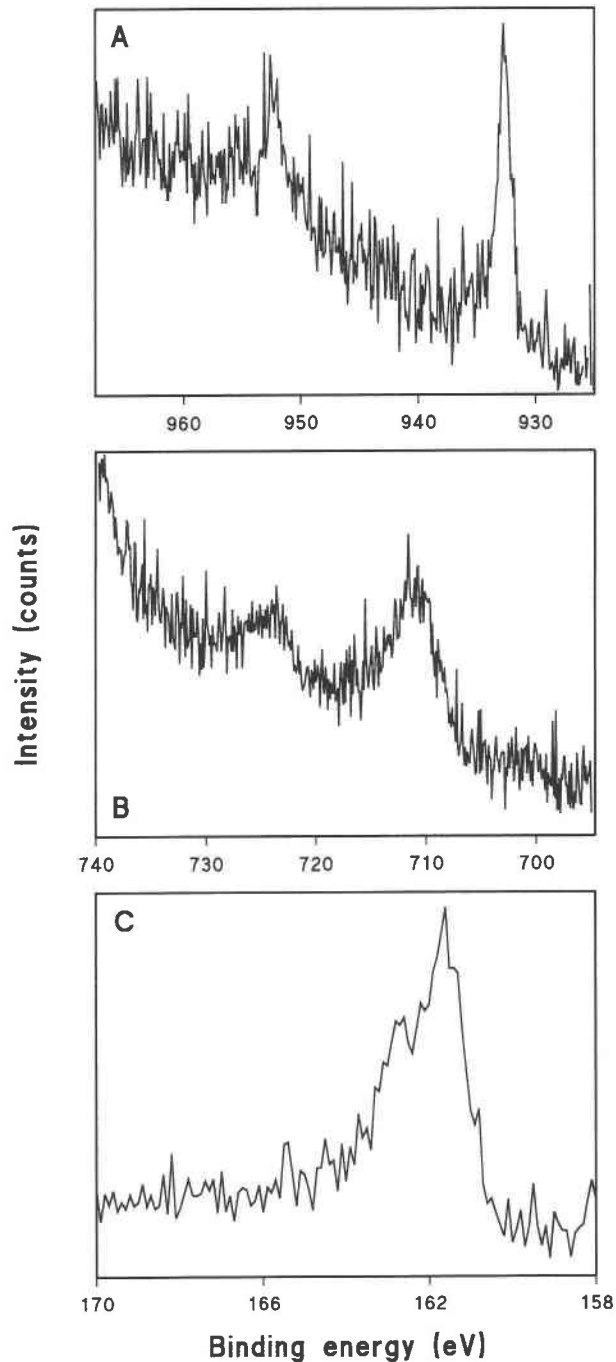
Figure 5 shows a set of current (density)–time transients in response to a step in electrode potential from rest value(s) to 0.4 V vs. S.C.E. in 0.1 M borax solution.
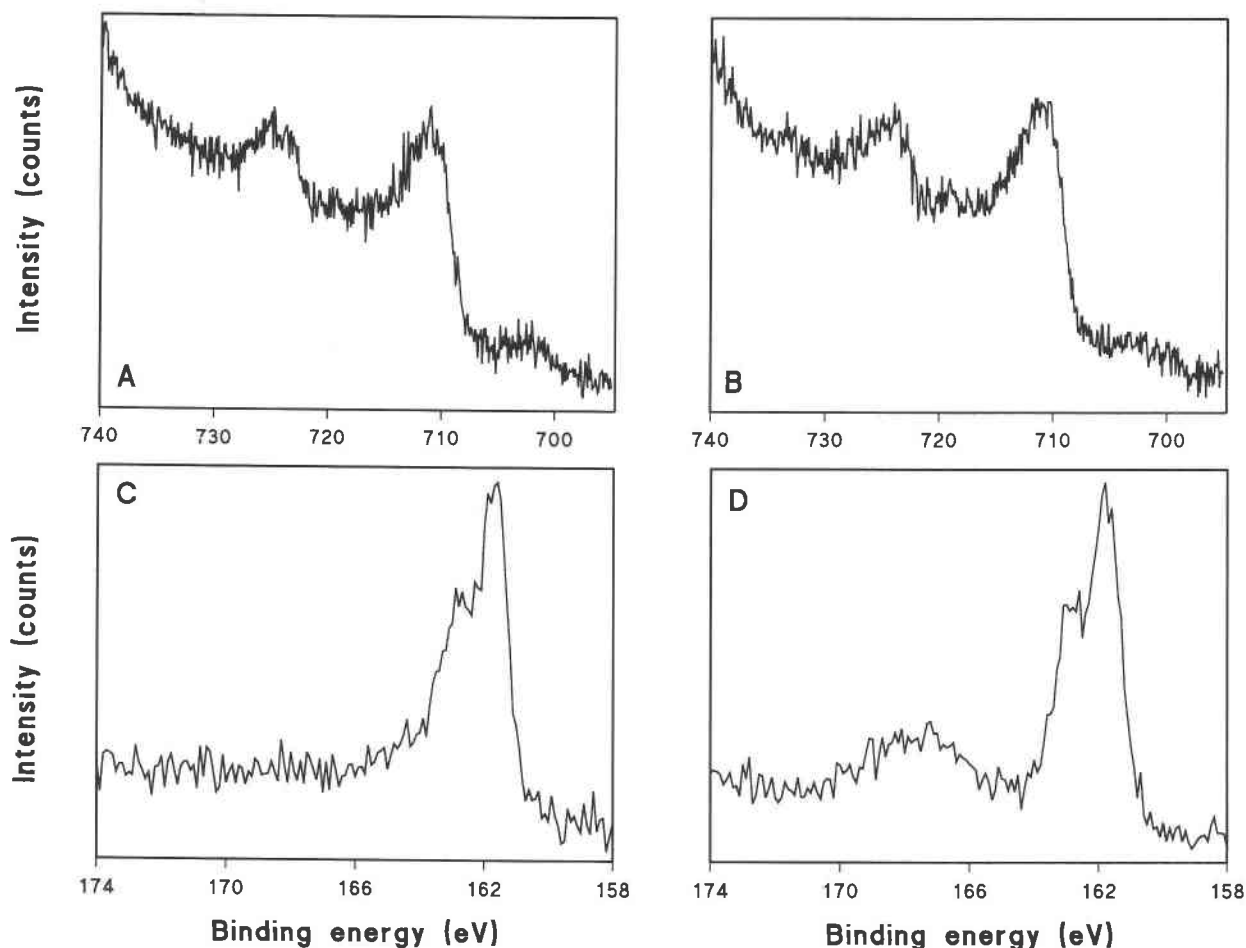
Fig. 9. XPS spectra from haycockite electrode surface oxidized in 0.1 M $Na_2B_4O_7$ at 298 K: (A) Fe 2p, oxidized at 0.1 V vs. S.C.E. with the passage of 96 C/m² over 170 min; (B) Fe 2p, oxidized at 0.4 V vs. S.C.E. with the passage of 92 C/m² over 49 min; (C) S 2p, oxidized at 0.1 V vs. S.C.E. with the passage of 96 C/m² over 170 min; (D) S 2p, oxidized at 0.4 V vs. S.C.E. with the passage of 92 C/m² over 49 min.

They indicate that, when oxidized potentiostatically, the relative oxidation rates of chalcopyrite, haycockite, and mooihoekite are time dependent. The oxidation rate of chalcopyrite is initially lower than that of haycockite and of mooihoekite. However, after approximately 40 and 150 s, the oxidation rate of chalcopyrite becomes slightly greater than that of mooihoekite and haycockite, respectively. Such a change suggests that, in the 0.1 M borax solution, the metal oxide oxidation products, particularly the iron oxide, play a vital role in the passivation. This is reasonable considering that copper and iron oxides have the lowest solubility at a pH of around 9 (i.e., 10^{-8} and 10^{-12} M for copper and iron oxides, respectively).

The data in Figure 5 were integrated to give oxidation charge densities, which increased approximately linearly with the square root of time, as shown in Figure 6. This suggests that the solid-state ionic transport (i.e., diffusion and migration) of Fe may be the rate-determining step in the oxidation, once the Fe surface sites have been oxidized. Moreover, from the slopes of the plots in Figure

6, it can be deduced that the transport rate of Fe ions in haycockite is approximately 12 times as fast as in chalcopyrite. This can be taken as evidence that interstitial transport rather than substitutional transport is the mechanism of Fe ion transport in the chalcopyrite and haycockite lattices. If the transport of Fe ions in chalcopyrite and haycockite accords with a substitutional mechanism, a small variation in chemical composition will not affect the transport rate so significantly. However, the interstitial mechanism could give a reasonable explanation for the experimental results and for the fact that, among Cu-Fe-S compounds, those with extra stuffed metal ions (haycockite, mooihoekite, and talnakhite) display a much higher transport rate than chalcopyrite.

X-ray photoelectron spectroscopy (XPS)

Figures 7 and 8 show the XPS spectra from a synthetic chalcopyrite electrode and a haycockite electrode, respectively. Both were oxidized in 1 M $HClO_4$ at 0.3 V vs. S.C.E. and 298 K for 100 s. Comparison of the spectra

in Figure 7 with those for the unoxidized phase, indicates that there was no significant shift in the binding energies of the Cu 2p, Fe 2p, and S 2p electrons after the chalcopyrite was oxidized potentiostatically at 0.3 V vs. S.C.E., suggesting that the change in the composition of the chalcopyrite surface was very slight. This is consistent with the observation that the oxidation rate of chalcopyrite at an electrode potential of 0.3 V vs. S.C.E. is very low, so that a charge density of only 14.2 C/m^2 was passed over 100 s. If the reaction were given by Equation 1, with $y = 1$ and two electrons produced per chalcopyrite molecule oxidized, it would correspond to the oxidation of about eight monolayers or an alteration depth of about 4 nm. Therefore, the Fe ions could be transported from the bulk lattice to the solid-electrolyte interface without resulting in a significant change of the chalcopyrite surface. On the other hand, comparison of the spectra of the unoxidized phase with those in Figure 8 indicates that, after the haycockite electrode is oxidized in 1 M $HClO_4$ at 0.3 V vs. S.C.E. for the same time, the Cu $2p_{3/2}$ peak position does not shift obviously, but the Fe $2p_{3/2}$ peak position shifts to a position of higher binding energy (712 eV), indicating the presence of adsorbed Fe^{3+} species. A charge density of 174 C/m^2 was passed over 100 s; if the reaction were again given by Equation 1, with $y = 5$ and ten electrons produced per haycockite molecule oxidized, it would correspond to oxidation of about 18 monolayers or an alteration depth of about 42 nm. In the S 2p spectrum obtained from the oxidized haycockite electrode, it can be seen that the binding energy of the peak is shifted to a higher value but does not reach the value of 164 eV expected for elemental S, suggesting that elemental S is not formed.

Hence, the spectra in Figures 7 and 8 support the view that, in the pre-wave region, the oxidation of Cu-Fe-S compounds in 1 M $HClO_4$ is through Reactions 1 and 2, i.e., that Fe is oxidized preferentially to Fe^{2+}, or, at electrode potentials > 0.53 V vs. S.C.E., Fe^{3+} ions, whereas Cu and S remain in the form of $Cu_xS_z^*$. The spectra also suggest that the transport of Fe ions in haycockite is faster than in chalcopyrite, and so after chalcopyrite and haycockite are oxidized under the same conditions, more $Cu_xS_z^*$ and Fe^{3+} species are formed and retained at the electrode surface.

Figure 9 shows the Fe 2p and S 2p spectra from haycockite oxidized in 0.1 M borax at electrode potentials of 0.1 and 0.4 V vs. S.C.E., respectively, with corresponding charge densities of 96 C/m^2 passed in 170 min and 92 C/m^2 in 49 min. If Reactions 5 and 6 were operative at 0.1 V vs. S.C.E., with $y = 5$ and 15 electrons per molecule of haycockite oxidized, this corresponds to the oxidation of about seven monolayers or an alteration depth of about 15 nm. For 0.4 V vs. S.C.E., uncertainties over the proportion of the current producing elemental S by Reaction 10 or sulfate by Reaction 11, preclude a similar analysis. The two Fe 2p spectra appear very similar with the binding energy of the $2p_{3/2}$ peak at around 712 eV, indicating that, at electrode potentials both of 0.1 and 0.4 V vs.

S.C.E., Fe is oxidized to Fe_2O_3. However, in the S 2p spectra, there is a clear difference between the haycockite oxidized at 0.1 V and at 0.4 V vs. S.C.E., i.e., when haycockite is oxidized at 0.4 V vs. S.C.E., some extra features occur in the spectra at a binding energy of about 166–170 eV (Fig. 9D), suggesting that some iron or copper sulfate is formed.

REFERENCES CITED

Ammou-Chokroum, M., Cambazoglu, M., and Steinmetz, D. (1977) Oxidation menagee de la chalcopyrite en solution acide: Analyse cinetique des reactions: I. Modeles chimiques. Bulletin de la Société française de Minéralogie et de Cristallographie, 100, 149–161.

Ammou-Chokroum, M., Steinmetz, D., and Malve, A. (1978) Etude electrochimique de l'oxydation de la chalcopyrite en milieu acid chlorure. Bulletin de la Société française de Minéralogie et de Cristallographie, 101, 26–43.

Ammou-Chokroum, M., Sen, P.K., and Fouques, F. (1981) Electrooxidation of chalcopyrite in acid chloride medium, kinetics, stoichiometry and reaction mechanism. In J. Laskowski, Ed., Proceedings of the XIII International Mineral Processing Congress, Warsaw, Poland, 1979, p. 759–809. Elsevier Scientific, New York.

Cabri, L.J. (1967) A new copper-iron sulphide. Economic Geology, 62, 910–925.

Cabri, L.J., and Hall, S.R. (1972) Mooihoekite and haycockite, two new copper-iron sulfides, and their relationship to chalcopyrite and talnakhite. American Mineralogist, 57, 689–708.

Dean, F. (1991) Chalcopyrite photoelectrochemistry. Ph.D. thesis, University of London, London.

Gardner, J.R., and Woods, R. (1979) An electrochemical investigation of the natural flotability of chalcopyrite. International Journal of Mineral Processing, 6, 1–16.

Holliday, R.I., and Richmond, W.R. (1990) An electrochemical study of the oxidation of chalcopyrite in acidic solution. Journal of Electroanalytical Chemistry and Interfacial Electrochemistry, 288, 83–98.

Jones, D.L. (1974) The leaching of chalcopyrite. Ph.D. thesis, University of British Columbia, Vancouver, Canada.

Jones, D.L., and Peters, E. (1976a) Electrochemical experiments with chalcopyrite electrodes in aqueous solutions up to 200 °C. In High temperature high pressure electrochemistry in aqueous solutions, p. 443–458. National Association of Corrosion Engineers, Houston, Texas.

———(1976b) The leaching of chalcopyrite with ferric sulphate and ferric chloride. In Extractive metallurgy of copper II, p. 633–653. Transactions of the Metallurgical Society of AIME, New York.

McMillan, R.S., Mackinnon, D.J., and Dutrizac, J.E. (1982) Anodic dissolution of n-type and p-type chalcopyrite. Journal of Applied Electrochemistry, 12, 743–757.

Page, P.W. (1988) Electrochemical behaviour of pyrite, pyrrhotite, pentlandite and chalcopyrite. Ph.D. thesis, University of London, London.

Vaughan, D.J., and Craig, J.R. (1978) Mineral chemistry of metal sulfides (1st edition), 493 p. Cambridge University Press, Cambridge, U.K.

Warren, G.W. (1978) Electrochemical oxidation of chalcopyrite. Ph.D. thesis, University of Utah, Salt Lake City, Utah.

Warren, G.W., Wadsworth, M.E., and El-Raghy, S.M. (1982) Passive and transpassive anodic behaviour of chalcopyrite in acid solutions. Transactions of the Metallurgical Society of AIME, 13B, 571–579.

———(1983) Anodic behavior of chalcopyrite in sulfuric acid. In K. Osseo-Asare and J.D. Miller, Eds., Proceedings of the III International Symposium on Hydrometallurgy, AIME, Atlanta, Georgia.